A SPARSE RECONSTRUCTION ALGORITHM FOR PARALLEL SPIRAL MR SPECTROSCOPIC IMAGING

Ramin Eslami and Mathews Jacob

Department of Biomedical Engineering, University of Rochester, Rochester, NY 14627

ABSTRACT

In this paper we propose an efficient sparse reconstruction scheme for the parallel MRSI data acquired using a fast spiral scheme. We model the system using the MR priors estimated from the water reference scan. In our sparse reconstruction approach, we minimize the total variation and ℓ_1 norm of the compartmentalized MRSI data in order to reduce noise, inhomogeneity distortions, and spectral leakage. We demonstrate significant improvement for in vivo brain results when compared to classical regularized SENSE MRSI reconstruction.

Index Terms— Magnetic resonance spectroscopic imaging, sparse reconstruction, spiral sequence, total variation

1. INTRODUCTION

MR spectroscopic imaging (MRSI) is an in vivo molecular imaging scheme that provides the concentration distribution of various brain metabolites. It is emerging as a useful technique for the diagnosis of various diseases including cancer [12], epilepsy [3], and multiple sclerosis [4]. The main limitations of this scheme that restricts its clinical utility include its poor signal to noise ratio (SNR), low spatial resolution, and the poor spatial coverage associated with this scheme. The low spatial resolution introduces several artifacts such as partial voluming errors, spectral leakage from extra-cranial lipids, and line-shape distortions induced by magnetic field inhomogeneity. Good spatial coverage is often highly desirable in cancer imaging applications to detect metastases separated from the location of the main tumor.

Several fast scan imaging schemes that rely on time-varying gradients to rapidly acquire the k-space data have been proposed to improve the spatial resolution and coverage in a specified scan time. Echo-planar spectroscopic imaging (EPSI) [10], [7] and spiral MRSI schemes are the most popular fast-scan methods. Since non-Cartesian trajectories such as spirals oversample the k-space center, these schemes are reported to be more SNR efficient compared to the classical EPSI schemes.

Parallel MRI techniques have also been introduced to accelerate MRSI [13], [15]. These methods exploit the spatial diversity of the sensitivity patterns of phased array coils to undersample the k-space. The data is then recovered using reconstruction algorithms such as sensitivity encoding (SENSE) [6], [14]. The main challenge associated with all of these acceleration techniques is the loss in SNR. This is especially a huge concern in signal starved MRSI schemes, where the low metabolite concentrations translate to poor SNR. To obtain sufficient SNR to interpret the data, most of the above schemes rely on averaging the accelerated data at the expense of scan time.

Most of the current non-Cartesian (e.g. gridding) and parallel MRSI schemes (kSPA, SENSE) recover each temporal frame of the spatio-temporal data independently using 2-D image reconstruction techniques [5], [11]. The spectral information is then recovered from these 3-D dataset by evaluating a temporal Fourier transform. Since these methods decouple the recovery of the 3-D dataset into several simpler 2-D reconstruction problems, they have limited capability in exploiting the redundancy in the spatial spectral data to make the problem well-posed and hence minimize the SNR loss. The above decoupled strategy also makes it difficult to compensate for distortions induced by magnetic field inhomogeneity as well as spectral leakage artifacts.

We introduce a novel sparse reconstruction algorithm for the recovery of non-Cartesian parallel MRSI data to overcome the limitations of current reconstruction schemes. We pose the recovery of the entire 3-D dataset as a single optimization problem, which enables us to exploit the redundancy in the data and to compensate for the artifacts. Specifically, we regularize our reconstructions using the spatial total variation (TV) norm of the compartmentalized MRSI data. The 3-D reconstruction scheme also enables us to compensate for field inhomogeneity and T_2^* losses by incorporating their estimates from water reference data. We also model the spectral signal as a sparse linear combination of spikes and polynomials, which was introduced in our previous work [1]. Using this model, the MRSI data will be a better fit for the spatial TV scheme. In addition, we can significantly reduce the error amplification in the reconstruction by making the problem well-posed.

We acquire the k-space data using a spiral MRSI scheme with multiple spatial interleaves. Furthermore, we acquire the fully sampled data, which was retrospectively downsampled by skipping the interleaves. We demonstrate the utility of the proposed algorithm to significantly minimize the noise amplification in the reconstruction using numerical simulation and in vivo acquisition. We show that we can achieve a two-fold acceleration for the in vivo data acquired with multi-shot spiral trajectory and 12-channel head coil without significant loss in image quality. This enables us to reduce the scan time required for a single slice scan to 32s, which is a significant reduction compared to the ten-minute scan time required in our previous EPSI based sequence. Hence, the proposed work has potential to enable whole brain MRSI acquisitions in around eight minutes.

2. ACQUISITION SYSTEM

We designed a spin echo MRSI sequence based on the analytical spiral trajectory reported in [2] for the $3T$ Tim Trio Siemens scanner. The trajectory covers $N_x \times N_y \times N_f = 44 \times 44 \times 256$ of the k-space data for a FOV of $24 \times 24\text{cm}^2$ and slice thickness of 1cm resulting in a voxel size of $0.55 \times 0.55 \times 1\text{cc}$. We used 32 spatial interleaves with $TE = 40\text{ms}$ and $TR = 2\text{s}$. Therefore, the total scan time without acceleration is 64s. Each echo covers a spiral-out and the fly-back gradient to return the trajectory to the k-

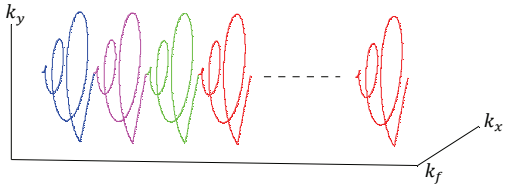

Fig. 1. A schematic plot of the MRSI spiral trajectory.

space center. The whole echo time is 1.32ms, which provides a bandwidth of 758Hz. Fig. 1 shows a schematic plot of the MRSI spiral trajectory for an interleaf.

For each interleaf, we used four analog-to-digital converters (ADC's), each covering 64 echoes. We start each ADC a few milliseconds earlier than the start of the next echo in order to avoid ADC's transient response during the readout.

In addition to the water-suppressed MRSI data, we also acquire a water reference scan with the same resolution from which we estimate field map, sensitivity maps (for the employed 12-channel head coil), and water and fat masks. For in vivo scans, we apply saturation bands to suppress fat. Nevertheless, we still use a fat mask in our reconstruction to reduce leakage from the unsuppressed lipid signals.

3. SPARSE RECONSTRUCTION

3.1. Image Formation

Ignoring the T_1 relaxation time, we model the discretized single-slice parallel MRSI acquisition scheme for a coil n_c ($n_c \in \{1, \dots, N_c\}$) when imaging $v[\mathbf{n}, n_f]$ as

$$\hat{s}\big[\mathbf{k}, k_f, n_c\big] = \underbrace{\sum_{\mathbf{n}=\mathbf{0}}^{\mathbf{N-1}} \sum_{n_f=0}^{N_f-1} e^{-j\omega_0[\mathbf{n}]k_f} e^{-k_f/T_2^*[\mathbf{n}]} e^{-j2\pi(\bar{\mathbf{k}}.\mathbf{n}+n_f\bar{k}_f)} \mathcal{S}[\mathbf{n}, n_c] v[\mathbf{n}, n_f]}_{\mathcal{A}v}. \quad (1)$$

Here $\omega_0 = 2\pi f_0 = \gamma \Delta B_0[\mathbf{n}]$ represents the field map in which $\Delta B_0[\mathbf{n}]$ is the field inhomogeneity, γ denotes the gyromagnetic ratio, and $\mathbf{n} = (n_x, n_y)$ is the spatial position in the slice. $\mathcal{S}[\mathbf{n}, n_c]$ denotes the sensitivity map for the coil n_c. The MRSI raw data for this coil $\hat{s}\big[\mathbf{k}, k_f, n_c\big]$ lie on the spiral trajectory $\mathbf{k} = (k_x, k_y) \in \Gamma$. Here $\bar{\mathbf{k}} = (k_x/N_x, k_y/N_y)$, $\bar{k}_f = k_f/N_f$, and we ignore the time required to scan each echo.

Since the trajectory is not on a Cartesian grid, we need to estimate the non-uniform Fourier coefficients on a uniform grid in order to use fast Fourier transform (FFT). In our implementation, we use the recently proposed optimized least square non-uniform FFT [8].

3.2. MRSI Reconstruction

To reconstruct the MRSI signal $v[\mathbf{n}, n_f]$ in (1), we take advantage of sparse nature of the MRSI data and propose to minimize spatial discrete TV norm of the signal using the following criterion

$$v = \arg\min_v \{\mathrm{TV}_{\mathbf{n}}(v)\}, \quad \text{s.t.} \quad \|\mathcal{A}v - \hat{s}\| \le \epsilon \|\hat{s}\|, \quad (2)$$

where the operator $\mathcal{A}$ denotes the system model as stated in (1). ϵ is chosen based on the standard deviation of the measurement noise. Note that in (2) we use the raw data $\hat{s}\big[\mathbf{k}, k_f, n_c\big]$ from all coil channels $n_c = 1, \dots, N_c$. We can reformulate (2) as

$$\tilde{v} = \arg\min_v \{\|\mathcal{A}v - \hat{s}\|^2 + \lambda \mathrm{TV}_{\mathbf{n}}(v)\}. \quad (3)$$

The spatial TV norm is defined as

$$\mathrm{TV}_{\mathbf{n}}(v) = \|\Delta_{\mathbf{n}} v\|_{\ell_1} = \sum\nolimits_{\mathbf{n}, n_f} \sqrt{|\Delta_x v|^2 + |\Delta_y v|^2},$$

where $\Delta_x v$ is the finite difference along the n_x dimension $\Delta_x v = v[n_x + 1, n_y, n_f] - v[n_x, n_y, n_f]$.

In order to reduce leakage and cross talks between different spatial regions in the MRSI data such as metabolites and the (remaining) fat signal, we propose to restrict the TV norm to only the water region Ω_1 [1] (so we update the TV norm as $\mathrm{TV}_{\mathbf{n}}^{\Omega_1}(v) = \|\Delta_{\mathbf{n}}^{\Omega_1} v\|_{\ell_1}$), and the MRSI signal v to the whole spatial region defined by the brain boundary $\Omega = \Omega_1 + \Omega_2$ that includes extra-cranial fat region Ω_2. Hence we rewrite the optimization problem (3) as

$$\tilde{v} = \arg\min_v \{\|\mathcal{B}v - \hat{s}\|^2 + \lambda \mathrm{TV}_{\mathbf{n}}^{\Omega_1}(v)\}. \quad (4)$$

Here $\mathcal{B} = \mathcal{A}\mathcal{M}_\Omega$ where $\mathcal{M}_\Omega$ is the masking operator defined as $\mathcal{M}_\Omega v = \begin{cases} v, & \mathbf{n} \in \Omega \\ 0, & \text{else} \end{cases}$.

Similar to our previous work [1], we model the MRSI spectral signal (in a region of interest (ROI) that contains metabolites peaks) as a linear combination of spikes and polynomials. This way, we sparsify the signal leading to a reduced TV norm that better fits to our model. Using sparsity criterion in our model, we make the problem well-posed especially when we apply undersampling.

We decompose the signal v using the union of Diracs and polynomials bases functions $\Phi = (\varphi \quad \psi)$ as

$$v = \Phi w = \underbrace{\varphi w_c}_{\text{baseline}} + \underbrace{\psi w_d}_{\text{peaks}},$$

and rewrite (4) as

$$\tilde{w} = \arg\min_w \{\|\mathcal{B}v - \hat{s}\|^2 + \lambda_1 \mathrm{TV}_{\mathbf{n}}^{\Omega_1}(w) + \lambda_2 \|w\|_{\ell_1}\}. \quad (5)$$

We added the ℓ_1 penalty in (5) to account for the spectral sparsity. Parameter λ_1 determines the level of smoothness of the reconstructed signal, whereas an appropriate selection of λ_2 secures proper decomposition of the signal into polynomials and spikes and helps to remove noise.

To find the system parameters for implementing the operator $\mathcal{B}$, we reconstruct the water reference scan using a variation of iterative SENSE reconstruction. We use Tikhonov regularization and OLS-NUFFT [8] in this scheme to reconstruct each channel and then we obtain sensitivity maps. Having the sensitivity maps, we form the reconstructed water MRSI data through the application of sum of squares. From the reconstructed water data, we estimate field map (ω_0), T_2^* decay, and the water and fat masks. In our model, we only compensate for the contribution of field map in T_2^*; that is, we compensate for T_2' decay where $1/T_2^* = 1/T_2' + 1/T_2$.

To implement the system model $\mathcal{A}$ for each channel n_c ($n_c \in \{1, \dots, N_c\}$), we use the following equation

$$\hat{s}\big[\mathbf{k}, k_f, n_c\big] = \mathcal{N}_\Gamma^{\mathcal{U}} \mathcal{W}_\alpha \mathcal{F}_{n_f} \{\mathcal{S}[\mathbf{n}, n_c] v\big[\mathbf{n}, n_f\big]\}. \quad (6)$$

Here, $\mathcal{F}_{n_f}$ denotes the DFT along spectral dimension n_f, $\mathcal{W}_\alpha$ applies $\alpha[\mathbf{n}, k_f] = e^{-j(\omega_0[\mathbf{n}] + 1/T_2^*[\mathbf{n}])k_f}$ as a point-wise multiplication, and finally $\mathcal{N}_\Gamma^{\mathcal{U}}$ denotes NUFFT operator which calculates the Fourier transform of the resulting signal on the spiral trajectory $\mathbf{k} \in \Gamma$ for all coil channels and time frames.

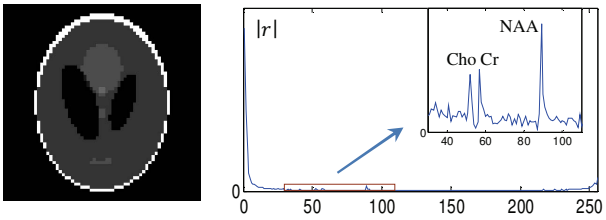

Fig. 2. *Left:* Shepp-Logan phantom. *Right:* Magnitude of the metabolite spectrum used in the simulation.

To accelerate the acquisition, we uniformly skip the interleaves. Thus, for instance, to achieve two times acceleration ($\times 2$), we only acquire interleaves $1,3,\ldots,31$. To reconstruct the undersampled data, we need to update the trajectory Γ in (6) with the used interleaves in the scan.

4. EXPERIMENTAL RESULTS

To test our sequence and the proposed parallel reconstruction algorithm, we acquired spiral MRSI data on a normal human subject. In addition, we carried out a numerical simulation to better benchmark our sparse reconstruction scheme. In all the experimental results, we compare our reconstruction to a Tikhonov regularized iterative SENSE reconstruction (referred as SENSE henceforth) in which we employed OLS-NUFFT [8], and restricted the MRSI data to the mask $\mathcal{M}_\Omega$. In this scheme, we correct for the inhomogeneity and remove the baseline (for the same ROI as the proposed scheme) after reconstruction followed by a spatial Gaussian apodization.

4.1. Simulation

In this simulation we used Shepp-Logan phantom $p[\mathbf{n}]$ at size 64×64 and made a simulated MRSI data $v[\mathbf{n}, n_f]$ with size $64 \times 64 \times 256$ by scaling and copying a reconstructed spectrum of a spectroscopy phantom $r[n_f]$ to all voxels of the Shepp-Logan phantom. Hence, we have $v[\mathbf{n}, n_f] = p[\mathbf{n}]r[n_f]$. As seen in Fig. 2, $r[n_f]$ has a high magnitude water peak and three peaks corresponding to metabolites Cho, Cr, and NAA.

We sampled v at a 64×64 spiral trajectory with 24 interleaves in the k-space to obtain $\hat{s}$. For this simulation we assumed a 12-channel coil and no inhomogeneity distortion. We used the sensitivity maps we had obtained from the in vivo scans and modified them to cover the whole phantom. For this simulation we assumed noisy measurements where we added random Gaussian white noise to $\hat{s}$ resulting in SNR of 29.5 dB.

We reconstructed the MRSI data using both proposed and SENSE reconstruction schemes with acceleration factors of $1, 2,$ and 4. In both methods, we adjusted regularizing parameters to suppress noise (and aliasing) while not oversmoothing the results.

Fig. 3 shows the reconstructed NAA peak image (only the inner region is shown for better visualization) as well as a sample spectrum with different acceleration factors. Improved reconstruction results for the proposed scheme especially with acceleration factors of $\times 2$ and $\times 4$ is clear. The proposed method could retrieve the peak image with more preserved details such as edges, and shows less noisy line shapes.

4.2. Human Brain

We acquired single-average MRSI data of a single slice of a brain from a healthy human subject with our MRSI spiral sequence using the parameters given in Section 2.

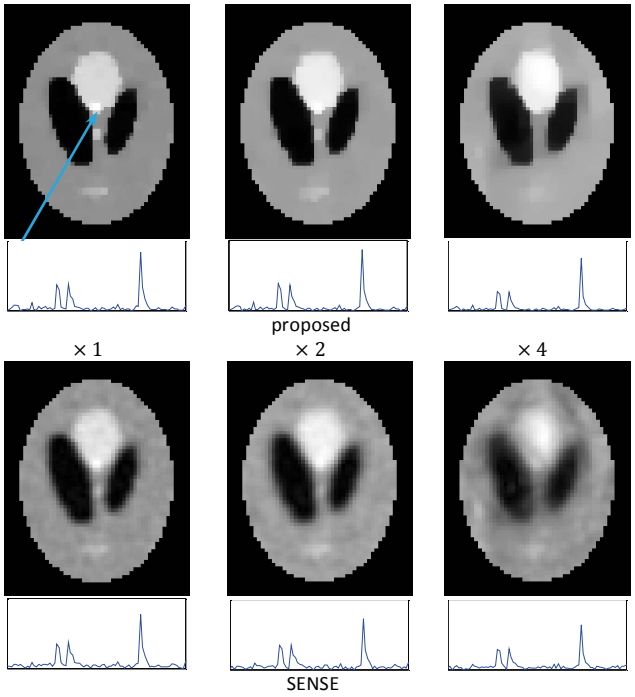

Fig. 3. Reconstructed NAA peak image along with a sample spectrum at the voxel shown by the arrow at different acceleration rates. Results using the proposed and SENSE approaches are shown at top and bottom, respectively.

In both the proposed and SENSE reconstruction schemes, we adjusted the regularizing parameters in order to suppress measurement noise while not oversmoothing the metabolite peak maps.

Fig. 4 shows the estimated field map and $1/T_2'$ for the brain scan. Here we used $T_2 = 74\text{ms}$ for the brain tissue [9]. As seen in this figure, there is strong inhomogeneity in the top region of the brain due to proximity to the frontal sinuses.

In Fig. 5 we depict the peak integral maps for the Cho, Cr, and NAA for both reconstruction schemes. Our proposed sparse reconstruction method is capable of recovering the signal even in areas with high inhomogeneity while it can retrieve details such as ventricles in the peak maps. In contrast, the SENSE approach shows losses in the top region of the brain and noisy reconstructions. In this figure, we also demonstrate the results with 2-fold acceleration. As seen, the proposed approach results in similar reconstructions as in the case of full sampling.

A few spectra at the voxels indicated by the dots are shown in Fig. 6. The improved reconstruction using the proposed approach leading to less noisy line shapes as well as restoring the spectra in the regions with high inhomogeneity is clear in this figure. Note

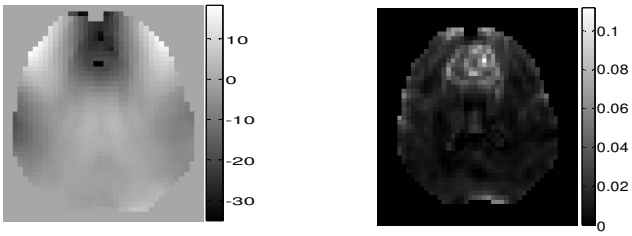

Fig. 4. *Left:* Estimated field map of the brain data in terms of Hz. *Right:* The estimated $1/T_2'$ for brain data (unit is ms^{-1}).

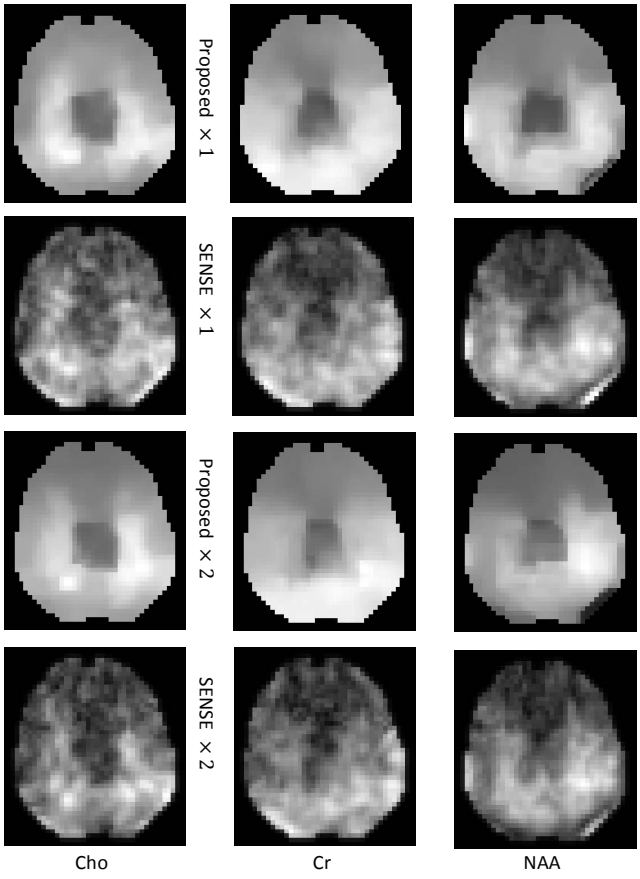

Fig. 5. Reconstructed peak integral maps of the brain metabolites using the proposed as well as SENSE schemes at acceleration rates of × **1** and × **2**.

that we achieve similar results for two times acceleration.

5. CONCLUSION

In this paper we proposed a novel sparse parallel MRSI reconstruction scheme based on a spiral trajectory. Taking advantage of the increased SNR offered by a 12-channel head coil, we were able to acquire the MRSI data in about 1min. We proposed a spatial TV reconstruction scheme in which we incorporated the estimated system model priors using the water reference scan. We also used a dictionary of polynomials and spikes in order to achieve sparser spectral MRSI signal for better restoration. Our brain in vivo results demonstrated significant improvement over the regularized iterative SENSE reconstruction.

6. REFERENCES

[1] R. Eslami and M. Jacob, "Robust reconstruction of MRSI data using a sparse spectral model and high resolution MRI priors," *IEEE Trans. Medical Imaging,* vol. 29, no. 6, pp. 1297-1309, Jun. 2010.

[2] G.H. Glover, "Simple analytic spiral k-space algorithm," Mag. Res. Med., vol. 42, pp. 412-415, 1999.

[3] W.A. Gomes, *et al.*, "Spectroscopic imaging of the pilocarpine model of human epilepsy suggests that early NAA reduction predicts epilepsy," *Mag. Res. Med.*, vol. 58, no. 2, pp. 230-235, 2007.

[4] O. Gonen, *et al.*, "Reproducibility of three whole-brain N-acetylaspartate decline cohorts in relapsing-remitting multiple sclerosis," *American J. Neuroradiology*, vol. 28, no. 2, pp. 267-271, Feb. 2007.

[5] M. Gu, C. Liu, and M. Spielman, "Parallel spectroscopic imaging reconstruction with arbitrary trajectories using k-space sparse matrices," *Mag. Res. Med.*, vol. 61, pp. 267-272, 2009.

[6] W.S. Hodge *et al.*, "A tour of accelerated parallel MR imaging from a linear systems perspective," *Concepts Mag. Res. Part A*, pp. 17-37, Sep. 2005.

[7] S. Hu *et al.*, "Compressed sensing for resolution enhancement of hyperpolarized 13C flyback 3D-MRSI," *J. Mag. Res.*, vol. 192, no. 2, pp. 258-264, Jun. 2008.

[8] M. Jacob, "Optimized least square non uniform fast Fourier transform (OLS-NUFFT)," *IEEE Trans. Signal Processing,* vol. 57, no. 6, pp. 2165-2177, Feb. 2009.

[9] Z.-P. Liang and P.C. Lauterbur, *Principles of magnetic resonance imaging: A signal processing perspective,* IEEE Press, New York, 2000.

[10] A.A. Maudsley *et al.*, "Mapping of brain metabolite distributions by volumetric proton MR spectroscopic imaging (MRSI)," *Mag. Res. Med.*, vol. 61, pp. 548-559, 2009.

[11] D. Mayer *et al.*, "Fast parallel spiral chemical shift imaging at 3T using iterative SENSE reconstruction," *Mag. Res. Med.*, vol. 59, pp. 891-897, 2008.

[12] T.R. McKnight, *et al.*, "Correlation of magnetic resonance spectroscopic and growth characteristics within Grades II and III gliomas," *J. Neurosurgery*, vol. 106, no. 4, pp. 660-666, 2007.

[13] S. Posse *et al.*, "Single-shot magnetic resonance spectroscopic imaging with partial parallel imaging," *Mag. Res. Med.*, vol. 61, pp. 541-547, 2009.

[14] K.P. Pruessmann, *et al.*, "Advances in sensitivity encoding with arbitrary k-space trajectories," *Mag. Res. Med.*, vol. 46, pp. 638-651, 2001.

[15] S.-Y. Tsai *et al.*, "Accelerated proton echo planer spectroscopic imaging (PEPSI) using GRAPPA with a 32-channel phased-array coil," *Mag. Res. Med.*, vol. 59, pp. 989-998, 2008.

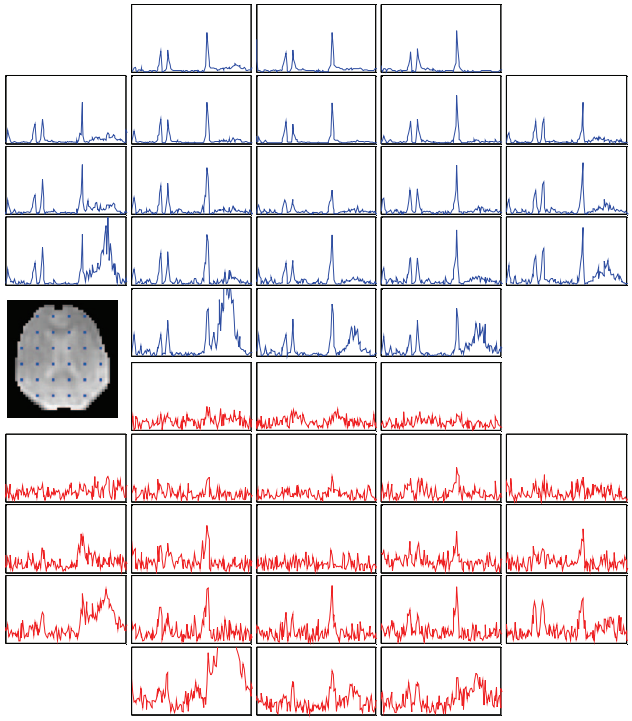

Fig. 6. A few spectra at the dotted voxels shown in the anatomy image using the proposed approach in top and SENSE reconstruction in bottom of the full sampled data.